

Dielectric Dynamics of Some Nylon 6/CaCO₃ Composites Using Broadband Dielectric Spectroscopy

G. M. Turkey,¹ A. M. Ghoneim,¹ A. Kyritsis,² K. Raftopoulos,² M. A. Moussa¹

¹Microwave Physics Department, National Research Center, Cairo, Egypt

²Department of Physics, National Technical University of Athens, 157 80 Athens, Greece

Received 1 September 2010; accepted 14 January 2011

DOI 10.1002/app.34166

Published online 13 June 2011 in Wiley Online Library (wileyonlinelibrary.com).

ABSTRACT: Broadband dielectric spectroscopy (10^{-1} to 10^6 Hz) in combination with TSDC were employed to study the relaxations and the conductivity phenomena in polyamide 6/CaCO₃ composites loaded with different contents and particle sizes of treated and untreated CaCO₃. In addition to the primary α -relaxation associated with the glass transition, significant interfacial relaxation and ionic conduction processes have been revealed. The temperature dependence of the relaxation rates of α -relaxation and Maxwell–Wagner–Sill-

er process as well as that of the hopping rate of the conduction mechanism were found to follow the Vogel–Fulcher–Tammann-model. This may support the idea that the three mechanisms are not completely independent. The modification of the filler does not add any effect on the resistivity values. © 2011 Wiley Periodicals, Inc. *J Appl Polym Sci* 122: 2039–2046, 2011

Key words: charge transport; dielectric properties; composites; heterogeneous polymers; molecular dynamics

INTRODUCTION

Nylon 6, which is widely used in the field of fibers and engineering plastics due to its excellent combination of good mechanical properties and easy processability,^{1–5} is a semicrystalline polymer and is rich in molecular dynamics that are influenced by its degree of crystallinity. Its composites and nanocomposites research has focused recently on the compounding and formulation in conjunction with post-processing materials properties and microstructural characterization. In general, there are a lot of well-known inorganic materials such as clay minerals, talc, mica, kaolin glass fibers, and calcium carbonate that have been successfully used as additives or reinforcement to improve the mechanical as well as the electrical properties of the polymers.^{5–12} The dielectric properties of nylons and their composites have received a wide attention, since these materials have quite complicated dielectric relaxation spectra reflecting their highly complex structure containing semicrystallinity, great strength of interchain force due to hydrogen bonding between amide groups as well as interphase interactions in their composites. The dielectric properties of Nylon 6 and Nylon 12 were reported very early, by Hirota et al.¹³ in 1966, on a frequency range between 100 μ Hz and 1 Hz. As expected, the more effective dynamics on this low

frequency range were the interfacial polarization at the boundaries between crystalline and amorphous regions, conductivity due to proton jump passing through hydrogen bonds, and an α -relaxation due to the segmental motion in the amorphous region. Above T_g , a space charge polarization mechanism due to the accumulation of charges at the crystalline-amorphous interfaces inside nylon's thin films was observed¹⁴ using thermally stimulated discharge technique that commonly works in ranges of equivalent frequencies of 10^{-2} to 10^{-4} Hz. In the meantime, the same technique in addition to the spectroscopy of dielectric relaxation and dynamic mechanical were widely used^{15–22} to probe the origin of the high and low temperature relaxation modes in Nylon 6 and the effect of moisture and crystallinity on the chain dynamics. In addition to the α -relaxation due to polymer segmental motion associated with the onset of the glass transition, another α' -relaxation was investigated.^{18,19} It was attributed to the water molecules and their intermolecular hydrogen bonding. The Maxwell–Wagner–Sillier (MWS) relaxation in Nylon 6 has been observed many years ago.^{17–20} Recently,²³ we have found a two step-like behavior in the investigations of ac conductivity measurements of Nylon 6 and its composites with CaCO₃ in dependence on frequency at relatively higher temperatures using RLC-meter (40 – 10^5 Hz). Lower frequencies investigations will give insight on the charge transport mechanism and lower temperatures will give us the opportunity to study the local dynamics. Because of its ability to probe molecular fluctuations and charge transport in a broad

Correspondence to: G. M. Turkey (gamalturky@yahoo.com).

frequency and temperature ranges, Broadband Dielectric Spectroscopy (BDS) turned out to be a useful experimental tool for probing charge transport in polymeric systems. BDS measures the complex dielectric function, ϵ^* , which is equivalent to the complex conductivity function, σ^* . This is expressed as $\sigma^*(\omega, T) = i\epsilon_0\omega\epsilon^*(\omega, T)$, implying that $\sigma' = \epsilon_0\omega\epsilon''$ (ϵ_0 being the vacuum permittivity and ω the radial frequency). In this study, two intermediate concentrations of two different particle sizes were chosen to investigate the effect of particle size and its loading on the different dynamic processes in the considered composite systems.

EXPERIMENTAL

Materials

The preparation of the investigated composites and the materials used are described in detail in a previous study by Moussa et al.²³ The Nylon 6/CaCO₃ composites was formed using melt blending method, with 4 and 6 wt % CaCO₃ powders in polyamide 6, in Brabender-like machine. The machine was heated to 503 K and Nylon 6 beads was added allowing the two screw revolving till the polymer completely melted, then the filler was added again allowing the two screw revolving for 3 min to enable homogeneous mixing. The samples were molded under high pressure press (30 MPa) to sheet of thickness 1.5 mm in stainless steel mold at 503 K with two Teflon papers sandwich the sample.

Treating CaCO₃ powders with oleic acid

The adsorption isotherms of oleic acid on the surface of CaCO₃ particles with 4 and 2 μ sizes were carried out from 0 to 0.1M solutions in toluene. Also, the effect of adsorbed amount on the sedimentation properties was recorded. This clarifies multilayer formation with just single chemically adsorbed layer. CaCO₃ powder was vigorously mixed with oleic acid solution using the optimum concentration obtained from both sedimentation and adsorption isotherm results. Allowing equilibrium concentration to be attained we waited for at least 48 h, then filtering, washing with toluene and allowing it to evaporate in open air, then in dry oven at 353 K for 2 h.

Abbreviation names of the samples

Since the samples have relatively long names, the priority needs for mentioning them. One can simplify the long name of each sample by coding them as shown in Table I below.

TABLE I
List of the Investigated Samples

No.	Sample name	Code
1	Blank Nylon 6	N
2	4% of unmodified 4 μ CaCO ₃	1B
3	6% of unmodified 4 μ CaCO ₃	1C
4	4% of modified 4 μ CaCO ₃	2B
5	6% of modified 4 μ CaCO ₃	2C
6	4% of unmodified 2 μ CaCO ₃	3B
7	6% of unmodified 2 μ CaCO ₃	3C

Dielectric relaxation spectroscopy

Complex dielectric function $\epsilon^* = \epsilon' - i\epsilon''$ as well as conductivity was measured by means of an Alpha Analyzer (Novocontrol GmbH, Hundsagen Germany). Temperature was controlled with accuracy better than 0.5 K by a Quattro Cryosystem manufactured by the same company. Specimens used, were of square shape with a surface of $\sim 30 \times 30$ mm and thickness of the order of mm. To form the capacitor, circular brass electrodes of diameter 20 mm were utilized. Measurements were carried out isothermally in the temperature range 123–473 K in steps of either 10 K (below 223 K) or 5 K (above 223 K) and in the frequency range 10^{-1} to 10^6 Hz.

Thermally stimulated depolarization currents (TSDC)

TSDC is a special dielectric technique in the temperature domain, which corresponds to measuring dielectric losses as a function of temperature at fixed low frequencies in the range (10^{-4} to 10^{-2} Hz).² Owing to its low equivalent frequency, it is characterized by high resolving power.^{24,25}

By this technique, the sample is placed in a capacitor and heated to a temperature T_p , where a dc field of the order of several hundreds V/m is applied for time t_p , which is by orders of magnitude higher than the relaxation time of the investigated mechanisms. With the field still applied, the sample is cooled at a steady rate to a low temperature T_d , where the relaxation times of the mechanisms are higher than the experimental time. The field is switched off, the capacitor is short circuited with a sensitive electrometer, and the sample is heated at a constant rate b , while the depolarization current is recorded by the electrometer.

In our study, the capacitor was formed as in DRS experiments, $T_p = 333$ K, dc voltage $V = 1$ kV, $T_d = 123$ K, $b = 3$ K/min.

RESULTS AND DISCUSSION

Figure 1 shows the dielectric loss as a function of frequency at two fixed temperatures (a) 233 K and

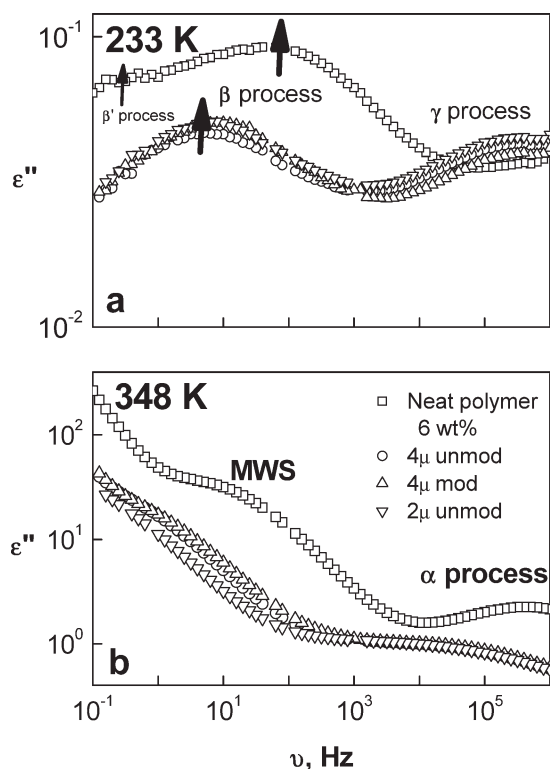


Figure 1 Dielectric loss, ϵ'' , of the considered composites versus frequency, ν , at two different temperatures: (a) lower temperature (233 K), (b) higher temperature (348 K).

(b) 348 K, for the neat polymer as well as three different composites with the same filler content (6 wt %). More than four dynamics could be observed in this figure. At lower temperature, Figure 1(a), one can see a broad dynamic relaxation (γ -relaxation) at higher frequencies. This dynamic was attributed to the fluctuations of the amide group with short segment of CH_2 sequences.^{16,18,19} By the addition of the filler, the γ -peak shifted remarkably toward lower frequency (became slower). It is, for Nylon 6, out of the considered frequency window. There is no remarkable effect of the particle size or the treatment of the filler surface on the peak position. At lower frequencies, a more intense and sharp peak namely, β -process, is observed. The peak position is shifted by more than one decade toward lower frequency by adding the filler whatever its size or if it is treated. At higher temperatures, Figure 1(b) shows α -relaxation process associated with the glass transition at higher frequencies followed by an interfacial polarization peak of MWS overlaid by conductivity contribution in decreasing frequency. Both former processes became broader and shifted toward lower frequency on the addition of the filler.

The isochronal graph, Figure 2, illustrates the dependence of the imaginary part of the complex dielectric permittivity ϵ'' on temperature for the neat Nylon 6 (N) and the sample, 1B (4% of unmodified

4 μ CaCO_3), as a function of temperature at a spot point frequency 1 kHz. All relaxation dynamics as well as charge transport can be identified in both the composite and the pure polyamide 6. These relaxations were previously identified and reported for the pure polyamide 6.^{26–28} The figure shows the effect of addition of the highest average particle size of CaCO_3 powder (4 μ) within the moderate percent on the dynamic behavior of the neat polyamide 6. This gives results similar to the effect of drying the neat polyamide 6 as shown by Laredo et al.¹⁹ All processes are shifted to higher temperature on the addition of the filler as expected. The lowest temperature process at about 173 K is the so-called γ -process. In increasing temperatures, another secondary relaxation peak appears at about 253 K that is called β -process. There is a number of varying opinions existing in the literature regarding the origin of this dynamic. Frank et al.¹⁶ attributed the β -relaxation to the movement of more extended CH_2 segments as well as motions of the amide groups. These motions are exacerbated by the presence of water in the system. Laredo et al.¹⁹ believe that the β -relaxation is due solely to firmly bound water that is often present in polyamides despite drying and can be completely eliminated only by extremely rigorous drying procedures. In the review by McCrum et al.,²⁹ the dielectric β -relaxation was attributed to NH_2 and OH chain end group movements, while others attributed it to the motion of a water polymer complex.²⁹ The higher temperature peak appears at about 328 K that is close to the glass-rubber transition temperature obtained by DSC, called α -process is connected with the onset of large-scale motions of the chain segments. The highest temperature process that appears at about 393 K is attributed to the interfacial polarization called MWS relaxation.⁶

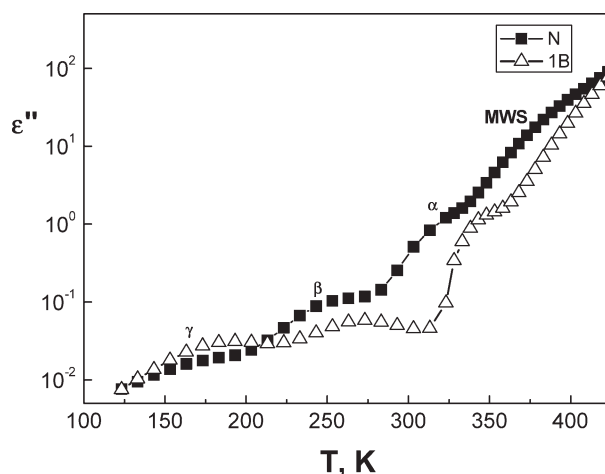


Figure 2 The temperature dependence of ϵ'' for the neat sample N and the composite 1B at spot frequency point 1 kHz.

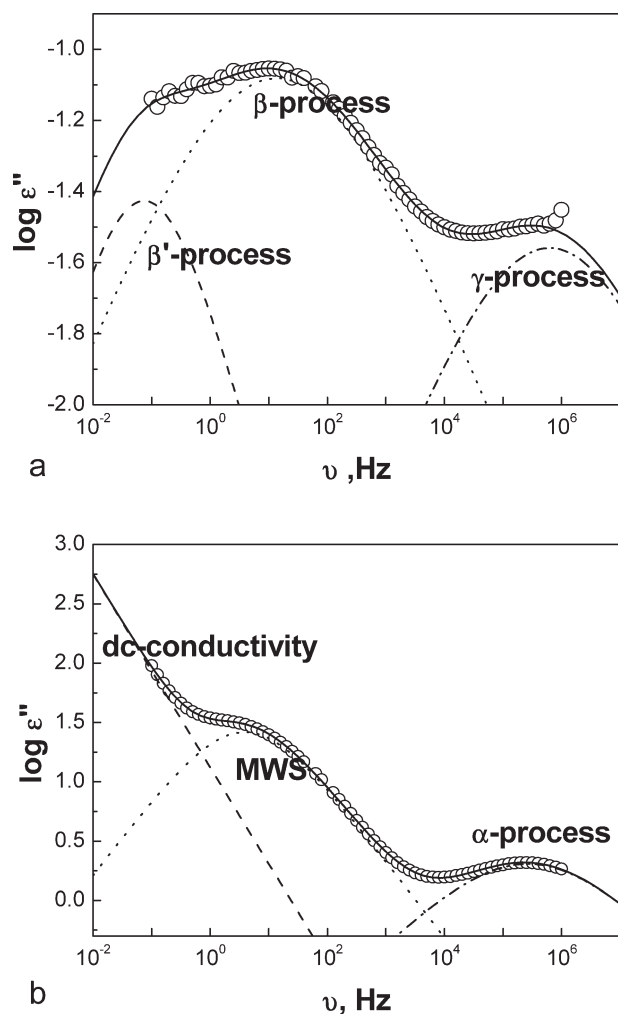


Figure 3 Separation of the dynamic peaks for the neat Nylon 6 at (a) 223 K and (b) 343 K. Lines are fit of HN-equation.

The study and analysis of the isothermal data enable detailed study of each relaxation process. The relaxation rate at maximal loss (mean relaxation rate), v_{\max} is extracted by fitting the following model function of Havriliak–Negami on the data.

$$\varepsilon^* = \varepsilon_{\infty} + \frac{\Delta\varepsilon}{\left(1 + \left(i\frac{\nu}{\nu_0}\right)^{1-\alpha}\right)^{\beta}} \quad (1)$$

In this expression, ν_0 is the characteristic frequency of the relaxation, ε_{∞} is the dielectric response at frequencies $\nu \gg \nu_0$, $\Delta\varepsilon$ is the dielectric strength, that is, the contribution of the relaxation to the static dielectric permittivity, while α and β are shape parameters expressing the broadening and asymmetry of the peak with respect to Debye model respectively. (For Debye relaxation $\alpha = 0$ and $\beta = 1$). For $\beta = 1$, the equation reduces to the symmetric Cole–Cole model, which is known to apply for local

secondary relaxations. α -relaxation is known to be asymmetric; however, due to the strong overlapping with other relaxations, studying asymmetry led to ambiguous results, therefore Cole–Cole model was utilized for segmental α -relaxation, too.

Figure 3(a) clarifies the existence of three relaxation processes in this frequency range at that relatively low temperature (223 K). Also analyzing the dependence of imaginary part of the complex dielectric permittivity, ε'' , on frequency at 343 K [Fig. 3(b)] shows the effect of dc conductivity, MWS process, and α -relaxation process in the order of increasing frequency. Figure 4 shows the activation plot obtained by fitting with HN-equation to the data. The obtained results of the relaxation rate as a function of the temperature follows Arrhenius equation:

$$\log v_p = \log v_{\infty} - \frac{(\ln 10)E_A}{K_B T} \quad (2)$$

where v_p is the frequency of maximal loss or the relaxation rate of the dynamic process, $v_{\infty} = \frac{1}{2\pi\tau_{\infty}}$ the relaxation rate in the high temperature limit, E_A the activation energy and K_B the Boltzmann constant. From this equation, the activation energies for the three relaxation processes at lower temperatures γ , β , and β' were found to be 0.341, 0.720, and 0.728 eV, respectively. On the other hand, α and MWS-relaxation processes were found to follow Vogel–Fulcher–Tammann (VFT) equation:

$$v(T) = \frac{1}{2\pi\tau(T)} = v_{\infty} \exp\left[\frac{-DT_0}{T - T_0}\right] \quad (3)$$

D is a constant and T_0 denotes the Vogel temperature (some times called the ideal glass transition temperature).

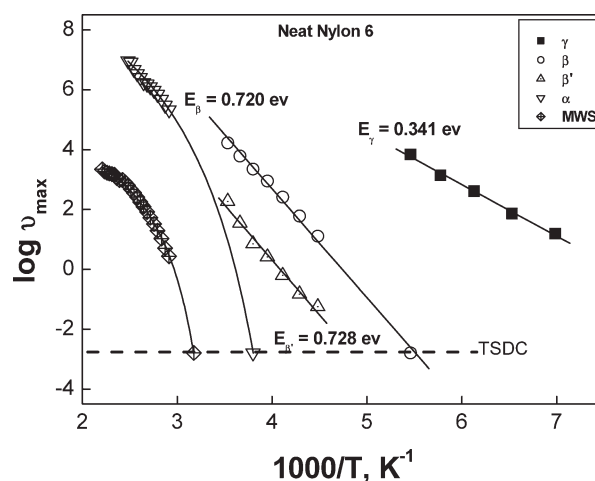


Figure 4 Activation plot of the neat Nylon 6 for γ , β , β' , α and MWS processes. The results of γ , β , β' follow the Arrhenius equation, while α and MWS were fitted with VFT equation.

Considering the relationship between the α -relaxation and the β' -relaxation, which disappeared for all the investigated composites, a close inspection on Figure 4 shows that both processes merge at higher temperatures and form the so-called $\alpha\beta$ - or α -process. It was called Williams process since it was first discussed by Graham Williams and his co-workers.^{30,31} With decreasing temperatures, both processes will separate from each other in a certain temperature region called splitting region according to Donth and coworkers.^{32–35} This scenario is assured according to the relaxation rate at maximal loss at very low frequency determined for α -process using TSDC technique that deviates remarkably from that of the β -process.

Effect of the filler on the dynamic of polyamide 6

There are numerous effects, since one observes four or even five peaks for the neat sample and the composites, respectively. One can study the effect on each process separately.

γ -process

The relaxation peak of this relaxation has more intensity for the composite than that of the neat Nylon 6 and is shifted toward lower frequencies (higher temperatures). The effect of adding the inorganic filler to the neat polymer seems to be similar to the effect of drying the wet sample of neat Nylon 6 obtained by Laredo et al.¹⁹ This behavior can be explained on the origin responsible for this dynamic process. It is related to the rotational motion of amide group with short segment of CH₂ sequences as previously mentioned. But one can think about cooperative rotational motion of N–H and C=O without any accompanying CH₂ sequences, since the decrease in the dipoles intensity by hydration is due to tightly bound water molecules that join two carbonyl groups and so hinder mobility while shifting to a higher temperature due to firmly adsorbed water molecules or due to the interaction of this dipoles with water molecules present in the polymer matrix. One can assume that CaCO₃ disturb hydrogen bonds formed between carbonyl groups (CO) and the amine groups (NH) so increase the number of reorienting dipoles, and hence increase the length of moveable CH₂ sequences, which explain the shift to higher temperature.

β -process

β -process has lower intensity for the composite than that of the neat Nylon 6—in opposite trend to the former process—also shifted toward lower frequencies. From the literature, this process is attributed to

the dynamics of firmly adsorbed water with amide groups through hydrogen bonding. The modification should lead to reducing or even disappearing of the relaxation peak that is not the case considering the modified and unmodified samples. In the review by Williams and Watts,³⁰ the dielectric β -relaxation was attributed to –NH₂ and –OH chain end group movements by some groups, based on this mechanism CaCO₃ can form hydrogen bonds with both types of chain end groups, and hence decrease the number of movable dipoles relate to this process. The small shift to higher temperature, more symmetry, and less broadening of the peak due to CaCO₃ particles bonded in majority to the longer polymer chain. In our opinion, this process is due to C–N bond of the amide group with accompanying of CH₂ sequences, and hence we explain the decrease in the number of reorienting dipoles by the interaction of CaCO₃ particles with the amide groups that have no adsorbed water molecules, so, the process appears due to only C–N of the amide group that have firmly adsorbed water molecules and so shift the peak to higher temperature.

α -process

The position of α -process relates to the onset of glass transition, cooperative motion of macromolecular chain. It appears in some other works^{6,19} as two peaks, the first process called plasticized one that was attributed to the glass transition and facilitated by hydration due to plasticization effect. The second one, called unplasticized process, was related to the glass transition, and is not affected by the hydration referring to the local modes. The coexistence of these two peaks seems to agree better with a representation of different spatial scales, that is, smaller cooperative rearrangement regions (CRR) sizes corresponding to faster modes, and larger CRR giving rise to slower ones. The addition of the inorganic filler reduces the intensity of the peak and also shifts its maximum position toward lower frequency (became slower). This effect is attributed to the unplasticization effect of CaCO₃. Even CaCO₃ decreases the degree of crystallinity, and its particles can serve as crosslinking of polymer chains.

MWS-process

Maxwell–Wagner–Sillars relaxation process relates to the interfacial polarization. This process thought to be due to the trapping of free charge carries at the boundaries between crystalline and amorphous regions. It is well known that the electrical conductivity of the crystalline phase is much lower than the conductivity of the amorphous phase in such semi-crystalline polymers. Free charge carriers (ions)

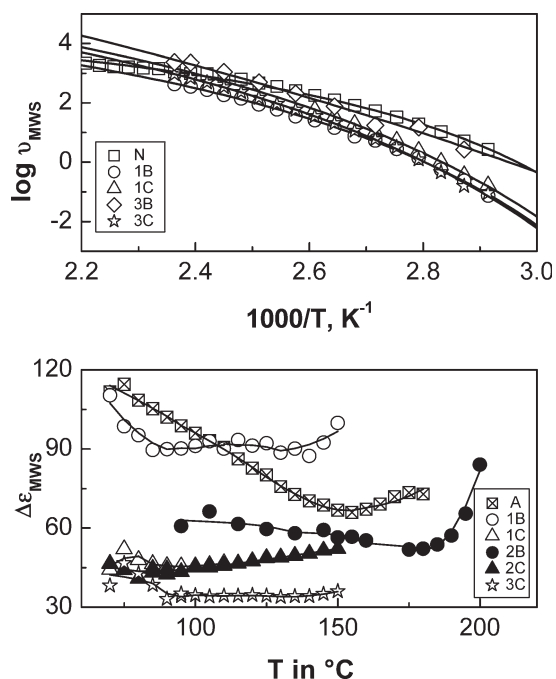


Figure 5 Maxwell-Wagner-Sillars process mean relaxation rate, $(v_{max})_{MWS}$ and dielectric relaxation strength, $\Delta\epsilon_{MWS}$ for the legend samples.

moving through the amorphous phase of the sample are hindered in their motion by crystalline domains. This reduces the conductivity at its frequency range and to be discussed later in the text. The model function HN, is fitted to the isothermal data of MWS dielectric relaxation peak to extract the relaxation rate at maximum loss, v_{MWS} , and the dielectric strength $\Delta\epsilon$. The characteristic frequency v_{MWS} and the dielectric strength $\Delta\epsilon$ of MWS relaxations are plotted against temperature for some selected samples to show the effect of concentration, modification, and the particle size of $CaCO_3$ and displayed in Figure 5. MWS relaxation is not only detected in the composite systems, but also found in the neat polymer. MWS effect in the neat semicrystalline nylons originates from protonic ion conduction through the two-phase crystal/amorphous solid that results in a polarization at the crystal/amorphous interface, which has been observed in Nylon 6 and other nylons.^{14,21,26} It is pointed out that v_{MWS} follows the VFT equation for all investigated samples. Figure 5 shows that MWS mechanism is faster at lower temperature for the neat polymer till the calorimetric glass transition and then became of comparable values with the different composites. Its dielectric strength decreases gradually till about 420 K and then is stabilized. There is clear coincidence between the dielectric strength of the unmodified and modified 4 μ composites at the concentration of 6 wt % (1C and 2C, respectively). The same concentration of 2 μ unmodified filler has the lowest values of dielec-

tric strength. This behavior reflected the higher degree of crystallinity of the neat Nylon 6 than that of the composites, so neat Nylon 6 has in general greater interfacial area between the crystalline and amorphous phases. But at higher temperatures, adsorbed water molecules in the amorphous phase will be degassed and allow the polymer chains to be ordered and increase the crystallinity at the expense of the overall interfacial area. However degassing of water molecules are also possible for the composite; the increase of crystallinity hindered by the presence of $CaCO_3$ particles due to the well-known unplasticizing effect of the filler.

Conductivity mechanism

Typical spectrum of the real part of complex conductivity, σ' , at different temperatures for the neat polymer is presented in Figure 6. It is well known that σ' —for highly conductive disordered polymers^{36–38} and many ion-conducting glass-forming liquids and glasses^{39–43} is characterized on the low frequency side by a plateau (the value of which directly yields the dc conductivity, σ_0) and a characteristic radial frequency, ω_c , at which dispersion sets in and turns into a power law ($\sigma \approx \omega^s$) at higher frequencies. Also, at lower frequencies, it was observed that σ' decreased from σ_0 value and this was attributed to electrode polarization that results from the interfacial effects attributed to the slowing down of charge carriers at the electrodes. The results obtained for the investigated samples (Figs. 6 and 7) exhibit a dc conductivity plateau σ_0 at lower frequencies for higher temperatures. There is no indication of the electrode polarization for such semicrystalline polymer or even for its composites. It is clear that σ_0 decreases and the characteristic radial

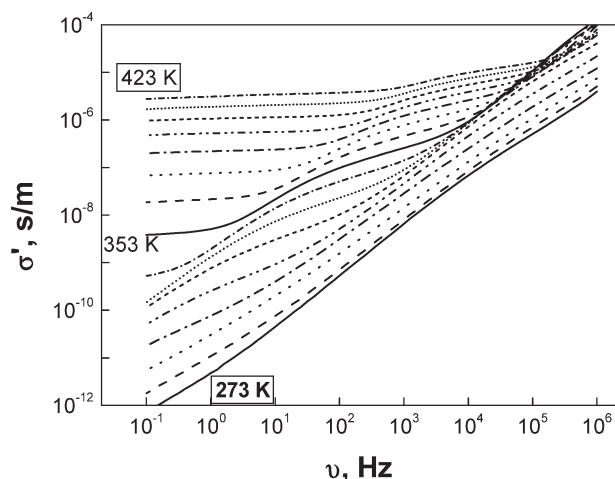


Figure 6 Real part of conductivity, σ' against frequency at temperatures from 273 to 423 K with 10 K increasing step for the neat Nylon 6, N.

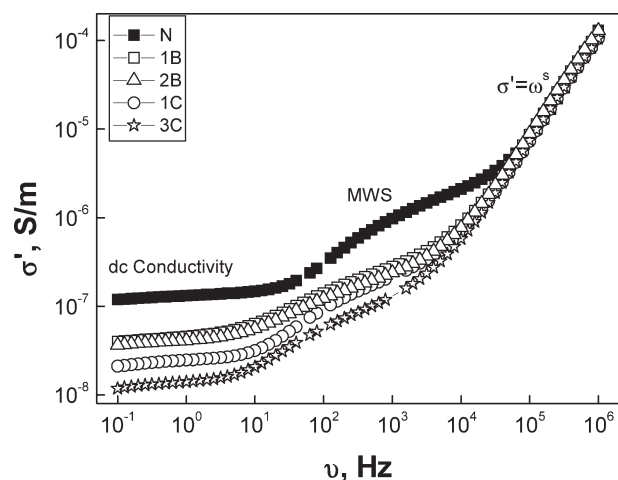


Figure 7 Real part of the conductivity, σ' against frequency at relatively higher temperature (378 K) for the neat Nylon 6, N, with samples 1B, 2B, 1C, and 3C.

frequency, ω_c , shifts toward lower frequencies with decreasing temperature. Figure 6 shows that the increase of temperature from 273 to 423 K increases σ_0 by about eight decades (from the order of 10^{-13} to 10^{-5}). This is due to the fact that as temperature increases, the degree of crystallinity decreases and the polymer chain acquires faster internal modes in which bond rotations produce segmental motion. This, in turn, favors hopping interchain and intra-chain ion movements and accordingly, the conductivity increases. On the other hand, at higher temperatures σ' is obeying the power law, ($\sigma \approx \omega^s$).

The conductivity curves also show a strong bend between the dc plateau and ac conductivity forcing the conductivity by another critical frequency. This phenomenon was observed previously in RCL-investigation and it is attributed to the MWS polarization.²³ Focusing now on the effect of filler modification and its content on the dc conductivity, σ_0 , Figure 7, clearly shows that the addition of the CaCO₃ generally reduces the conductivity of Nylon 6. However, no remarkable effect of modification on the dc conductivity is noticed here since there is coincidence for unmodified, (1B) and modified (2B) 4 wt % 4 μ CaCO₃. The main effect of the filler on the neat Nylon 6 is the unplasticizing, so it is assumed that the conductivity mechanism is mainly due to polymer chain movements that assist the migration of charge carriers. So, surface modification of the filler does not add any effect on resistivity values. Comparing now between different loading percentage of the filler, 1B: 4 wt % and 1C: 6 wt % of the unmodified 4 μ CaCO₃ samples and different particle size 1C: 4 μ and 3C: 2 μ of the unmodified filler at the same loading 6 wt % shows that the decrease in particle size and the increase of loading give more pronounced increase of resistivity.

The real part of the conductivity function $\sigma'(\omega)$ obeys the Jonscher's equation expressed as:

$$\sigma'(\omega) = \sigma_0 + A\omega^n = \sigma_0 \left[2 + \left(\frac{\omega}{\omega_c} \right)^n \right] \quad (4)$$

where ω_c is the characteristic frequency at which the real part of the conductivity begins to increase with

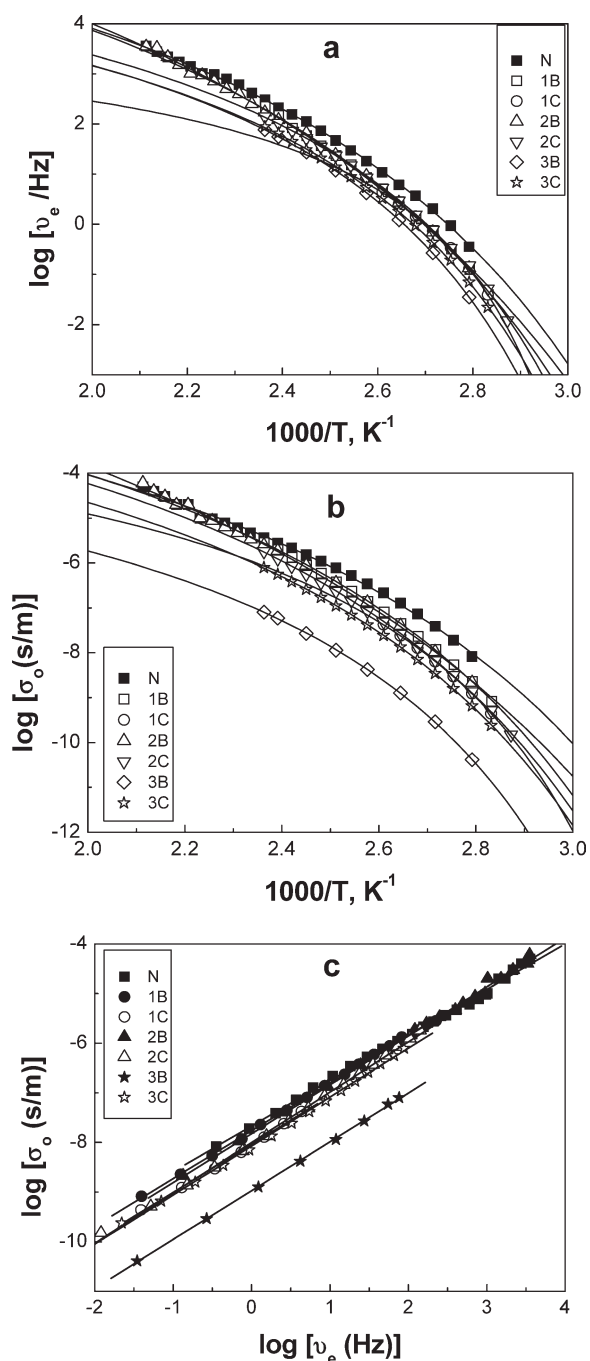


Figure 8 Temperature dependence of the characteristic charge transport rate, ν_e (a), dc conductivity, σ_0 (b) and σ_0 versus ν_e (c) for the legend samples. The solid lines are the fit of VFT (a and b) and linear relations (c).

frequency from the dc conductivity σ_o and n denotes power law exponent. The temperature dependence of both v_c and σ_o are illustrated graphically in Figure 8(a,b), respectively. Both obtained fit parameters follow the Vogel–Fulcher–Tamman dependence. This expresses an empirical scaling law relating the dc conductivity to the value of ω_c , known as the Barton–Nakajima–Namikawa (BNN) relation: $\sigma_o \sim \omega_c$ as given in Figure 8(c). The relation can also be stated as: $\sigma_o = p\varepsilon_0\Delta\varepsilon\omega_c$, where p is numerical constant, of order 1, ε_0 the permittivity of free space and $\Delta\varepsilon$ is the dielectric strength.

CONCLUSIONS

Based on the obtained data, one can concluded that

- Surface modification of CaCO₃ with oleic acid increases its compatibility with Nylon 6.
- Nylon 6 has four dynamic relaxation processes namely; γ , β , β' and α in addition to MWS polarization.
- γ , β , and β' processes obey Arrhenius activation equation, while α and MWS processes obey VFT activation.
- The additions of CaCO₃ to Nylon 6 shift all processes to higher temperatures in similar manner to drying the neat polymer.
- The strong bend in the conductivity curves is due to the strong dynamic MWS process.
- The shift of σ_o to lower values in the presence of CaCO₃ is higher for smaller size.
- The relation between σ_o and v_c obey BNN relation. So the $\Delta\varepsilon$ is temperature independent.

References

1. Kohan, M. I. *Nylon Plastics Handbook*; Wiley: New York, 1995.
2. Unal, H.; Mimaroglu, A. *J Reinf Plast Comp* 2004, 23, 461.
3. Unal, H.; Findik, F.; Mimaroglu, A. *J Appl Polym Sci* 2003, 88, 1694.
4. Kumar, A.; Ramanaiah, B. V.; Ray, A. R. *Polym Plast Technol Eng* 2006, 45, 1039.
5. Segatelli, M. G.; Yoshida, I. V.; Gonçalves, M. *Compos Part B Eng* 2010, 41, 98.
6. Noda, N.; Lee, Y.; Bur, A. J.; Prabhu, V. M.; Snyder, C. R.; Roth, S. C.; McBrearty, M. *Polymer* 2005, 46, 7201.
7. Unal, H.; Mimaroglu, A.; Alkan, M. *Polym Int* 2004, 53, 56.
8. Glenn, L. W.; Kim, H. C.; Miller, D. E.; Ellis, C. S. *J Reinf Plast Comp* 1998, 17, 901.
9. Hollin, J.; Miller, D.; Vautour, D. *J Reinf Plast Comp* 1998, 17, 1617.
10. Huang, D. D. *Polym Compos* 1995, 16, 10.
11. Takeda, N.; Song, D. Y.; Nakata, K. *Adv Compos Mater* 1996, 5, 201.
12. Takeda, N.; Ogihara, S.; Nakata, K.; Kobayashi, A. *Compos Interface* 1997, 5, 305.
13. Hirota, S.; Saito, Sh.; Nakajima, T. *Kollide-Zeitschrift und Zeitschrift für Polymere* 1966, 213, 109.
14. Gil-Zambrano, J. L.; Jubasz, C. *J Phys D Appl Phys* 1982, 15, 119.
15. Bizet, A.; Nakamura, N.; Teramoto, Y.; Hatakeyama, T. *Thermochim Acta* 1994, 237, 147.
16. Frank, B.; Frubing, P.; Pissis, P. *J Polym Sci Part B: Polym Phys* 1996, 34, 1853.
17. Gilzambrano, J. L.; Juhasz, C. *IEEE Trans Elect Insul* 1989, 24, 635.
18. Laredo, E.; Hernandez, M. C. *J Polym Sci Part B: Polym Phys* 1997, 35, 2879.
19. Laredo, E.; Grimau, M.; Sanchez, F.; Bello, A. *Macromolecules* 2003, 36, 9840.
20. McCall, D. W.; Anderson, E. W. *J Chem Phys* 1960, 32, 237.
21. Hanna, A. A. *Thermochim Acta* 1984, 76, 97.
22. Lehuy, H. M.; Rault, J. *Polymer* 1994, 35, 136.
23. Moussa, M. A.; Ghoneim, A. M.; Abdel Hakim, A. A.; Turky, G. M. *Adv Polym Technol* 2009, 28, 257.
24. Van Turnhout, J. In *Electrets, Topics in Applied Physics*; Sessler, G. M., Ed.; Springer: Berlin, 1980; Vol.33, pp81–215.
25. Kanapitsas, A.; Pissis, P. *Eur Polym Mater* 2000, 36, 1241.
26. Kapur, S.; Rogers, C. E.; Baer, E. *J Polym Sci Polym Phys* 1972, 10, 2297.
27. Rotter, G.; Ishida, H. *Macromolecules* 1992, 25, 2170.
28. Russo, P.; Acierno, D.; Di Maio, L.; Demma, G. *Eur Polym Mater* 1999, 35, 1261.
29. McCrum, N. G.; Read, B. E.; Williams, G. *Anelastic and Dielectric Effects in Polymeric Solids*; Dover: New York, 1991.
30. Williams, G.; Watts, D. C. *Nuclear Magnetic Resonance Basics, Principles and Progress, Vol. 4, NMR of Polymers*; Springer: Berlin Heidelberg, New York, 1997.
31. Kremer, F.; Schönhals, A. In *Kremer, F.; Schönhals, A, Broad-band Dielectric Spectroscopy*; Springer Springer-Verlag: Berlin Heidelberg, Germany, 2003, Chapter 7, p 254.
32. Garwe, F.; Schonhals, A.; Beiner, M.; Schoter, K.; Donth, E. *Macromolecules* 1996, 29, 247.
33. Garwe, F.; Schonhals, A.; Beiner, M.; Schoter, K.; Donth, E. *Phys Condens Matter* 1994, 6, 6941.
34. Donth, E. J. *The Glass Transition*; Springer: Berlin Heidelberg, New York, 2001.
35. Beiner, M.; Kahle, S.; Hemple, E.; Schoter, K.; Donth, E. J. *Europhys Lett* 1998, 44, 321.
36. Sangoro, J.; Turky, G.; Abdel Rehim, M.; Jacob, C.; Naumov, S.; Ghoneim, A.; Kärger, J.; Kremer, F. *Macromolecules* 2009, 42, 1648.
37. Turky, G.; Sangoro, J.; Abdel Rehim, M.; Kremer, F. *Polym Sci Part B Polym Phys*, 48 (2010) 1651.
38. Turky, G.; Shaaban Sh, S.; Schönhals, A. *J Appl Polym Sci* 2009, 113, 2477.
39. Roling, B.; Happe, A.; Funke, K.; Ingram, M. D. *Phys Rev Lett* 1997, 78, 2160.
40. Sidebottom, D. L. *Phys Rev Lett* 1999, 82, 3653.
41. Namikawa, H. *J Non-Cryst Solids* 1975, 18, 173.
42. Clacob, C.; Sangoro, J. R.; Serghei, A.; Naumov, S.; Korth, Y.; Kärger, J.; Friedrich, C.; Kremer, F. *J Chem Phys* 2008, 129, 234511.
43. Zielniok, D.; Eckert, H.; Cramer, C. *Phys Rev Lett* 2008, 100, 03590.